JOURNAL OF AIRCRAFT
Vol. 47, No. 4, July–August 2010

Design Optimization for Improved Soft In-Plane Tiltrotor Aeroelastic Stability in Airplane Mode

Jinho Paik* and Farhan Gandhi†
Pennsylvania State University, University Park, Pennsylvania 16802

DOI: 10.2514/1.43212

This paper examines the influence of parametric variation in individual rotor/wing design variables on whirl flutter stability improvements of a soft in-plane tiltrotor. This is followed by the use of formal gradient-based design optimization. The simulations are based on a full-scale soft in-plane Boeing model 222 rotor on a semispan wing. For this baseline configuration, the flatwise flexibility and chordwise flexibility are both outboard of the pitch bearing and produce destabilizing pitch-flap and pitch-lag couplings. The most influential rotor parameter in improving flutter stability characteristics is the distribution of flatwise flexibility vis-à-vis the pitch bearing, and large improvements are observed when flatwise flexibility is moved inboard. However, this can result in a large increase in lag frequency and turn the design into a stiff in-plane configuration. Using frequency constraints during optimization of rotor parameters and carefully selecting the airspeed range over which optimization is conducted results in improvement in subcritical wing mode damping and increase in critical flutter speed. Other rotor parameters changes that have some benefit are reduction in overall chordwise stiffness, positive increase in pitch-flap and pitch-lag coupling, and increase in control system stiffness. Wing design parameters are unable to increase the critical flutter speed but can improve the subcritical damping, primarily through an increase in wing torsion frequency and a simultaneous reduction in wing beam mode frequency. Optimization using a combination of rotor/wing design parameters yields a 35 kt increase in whirl flutter speed (from 390 to 425 kt) and an increase in subcritical damping from less than 1% to in excess of 2% critical.

Nomenclature

b	=	wing vertical bending (beam) mode
c	=	wing chordwise bending mode
$K_{P\beta}$	=	pitch-flap coupling parameter
$\tilde{K}_{P\beta}$	=	effective pitch-flap coupling due to blade flexibility
$K_{P\zeta}$	=	pitch-flap coupling parameter
$\tilde{K}_{P\zeta}$	=	effective pitch-lag coupling due to blade flexibility
K_β	=	blade flap stiffness
$K_{\beta B}$	=	blade flap stiffness outboard of the pitch bearing
$K_{\beta H}$	=	blade flap stiffness inboard of the pitch bearing
K_ζ	=	blade lag stiffness
$K_{\zeta B}$	=	blade lag stiffness outboard of the pitch bearing
$K_{\zeta H}$	=	blade lag stiffness inboard of the pitch bearing
R_β	=	fraction of flap flexibility outboard of pitch bearing
R_ζ	=	fraction of lag flexibility outboard of pitch bearing
t	=	wing torsion mode
x, y, z	=	hub translational degrees of freedom
$\alpha_x, \alpha_y, \alpha_z$	=	hub rotational degrees of freedom
β	=	blade flapping degree of freedom
β_P	=	rotor precone angle
ζ	=	blade lead-lag degree of freedom
φ	=	blade rigid pitch degree of freedom
ψ_s	=	azimuthal perturbation degree of freedom
$\omega_{\beta 0}$	=	nonrotating blade fundamental flap frequency
$\omega_{\zeta 0}$	=	nonrotating blade fundamental lag frequency
ω_φ	=	nonrotating blade pitch frequency (due to control system stiffness)

Received 13 January 2009; revision received 14 August 2009; accepted for publication 13 September 2009.

*Graduate Research Assistant, Vertical Lift Research Center of Excellence, Aerospace Engineering Department, 229 Hammond Building.

†Professor, Vertical Lift Research Center of Excellence, Aerospace Engineering Department, 229 Hammond Building. Associate Fellow AIAA.

I. Introduction

THE currently operating tiltrotors employ three-bladed, gimballed, stiff in-plane rotor systems (XV-15, V22, and BA609). While stiff in-plane rotor systems display reasonable aeroelastic and aeromechanical stability characteristics for tiltrotor aircraft, free of ground resonance, sufficiently high whirl flutter speeds (albeit with thick, high-stiffness wings) and adequate subcritical damping margins (before the flutter boundary), they develop significant in-plane dynamic hub loads, particularly during maneuvers, and this translates to structural weight and performance penalties. The loads would be an even greater problem for heavy-lift tiltrotor aircraft, bringing into question the feasibility of using stiff in-plane rotors on such aircraft. Because of lower load levels, soft in-plane rotor systems would be ideal candidates for future tiltrotor aircraft, especially for heavy-lift configurations. However, soft in-plane tiltrotors inherently have lower critical flutter speeds and reduced subcritical damping margins, compared to stiff in-plane tiltrotors. The few soft in-plane configurations that have been tested in a wind tunnel (Boeing model 222 [1] and the recent Bell Helicopter and U.S. Army semi-articulated soft in-plane rotor [2]) have exhibited unacceptably low levels of damping in the wing vertical bending mode. Furthermore, soft in-plane rotors can also be susceptible to aeromechanical instabilities (ground and air resonance). Therefore, ensuring adequate stability aeroelastic and aeromechanical stability characteristics is a prerequisite for soft in-plane rotor systems to be used in future tiltrotors.

There have been many previous studies that have examined the aeroelastic stability characteristics of tiltrotor aircraft in the airplane mode, and have focused on increasing the whirl flutter boundaries and the subcritical damping levels. The conventional approach to ensuring adequate whirl flutter stability margins has required wing structures with very high torsional stiffness [3]. This stiffness requirement leads to rather thick wing sections. The large aerodynamic drag associated with such thick wing sections is an obstacle to achieving the higher cruise speeds envisioned for future tiltrotor aircraft. It is therefore desirable to explore alternative methods for providing the required aeroelastic stability margins.

One approach to improve tiltrotor whirl flutter stability characteristics is the use of active control. During a wind-tunnel test of the Boeing model 222 soft in-plane rotor [1], a simple wing acceleration output feedback control system was successful in increasing the

damping of the poorly damped wing vertical bending mode. Johnson [4] analytically investigated the use of an optimal controller with an estimator for reduction of tiltrotor gust response for both the stiff and soft in-plane rotors. While [4] did not explicitly consider the problem of aeroelastic instability, it did confirm that active control was a feasible technique for tiltrotor damping augmentation. Studies by Nasu [5] and van Aken [6,7] analytically demonstrated the ability of a simple feedback control system using swashplate actuation to influence whirl flutter stability. More recently, a great deal of experimental work [2,8–11] has been performed jointly by NASA Langley Research Center and Bell Helicopter to evaluate the effectiveness of a modern adaptive control algorithm known as generalized predictive control for tiltrotor stability augmentation and vibration suppression.

References [12–14] have focused on wing-flaperon and swashplate actuation for damping augmentation and flutter boundary improvement for both stiff and soft in-plane tiltrotor configurations. These investigations have demonstrated the potential of a simple constant-gain output feedback controller, which is sensing easily measurable wing states in improving tiltrotor whirl flutter stability.

In some cases, the use of active control may be unavoidable to obtain desired whirl flutter stability characteristics, for example in the design of advanced rotor configurations for high-speed or heavy-lift tiltrotors. However, a passive design solution, if available, is certainly preferable. Furthermore, even if an active control approach is ultimately adopted, the uncontrolled system should be designed to be as stable as possible, easing the requirements on the active stabilization system.

Numerous studies have also focused on the influence of rotor and wing design parameters on whirl flutter stability. Hall [15] experimentally and analytically investigated the stability characteristics of the Bell XV-3. Reduced rotor pylon mounting stiffness was found to be destabilizing. Increased coupling between blade flapping and the rotor control system (δ_3 coupling) was also destabilizing. Young and Lytwyn [16] examined the influence of blade flap stiffness on stability and found that a fundamental flap frequency of approximately 1.1–1.2/rev provided the greatest stabilizing influence. However, Wernicke and Gaffey [17] pointed out that other design considerations such as blade loads and transient flapping response during maneuvers may preclude taking advantage of this ideal frequency placement for enhanced stability. Gaffey et al. [18] described the influence of various rotor and wing design parameters on aeroelastic stability, and also discussed the limits imposed on these parameters by other design constraints. Johnson [19,20] developed an analytical model that included elastic blade bending and torsion modes. The primary influence of blade torsion dynamics was reported to be a destabilizing pitch-lag coupling introduced to the rotor by blade flexibility outboard of the pitch bearing. Increased control system stiffness was shown to reduce the destabilizing effect.

More recent studies have continued to examine the influence of many different design parameters, including: rotor and wing stiffness properties [21], various kinematic couplings arising from hub and control system geometry [22], advanced geometry rotor blades (tip sweep, taper, and anhedral) [23], composite couplings in the wing [24,25] and rotor blades [21,25], and blade center of gravity and aerodynamic-center offsets [26–29]. Introduction of aeroelastic couplings into the wing and rotor has generally been reported to improve whirl flutter stability.

In the references cited above, the various parameters under consideration in each study were individually varied. The effect of simultaneous variation of multiple design variables has not been widely explored. Recently, in [30], formal design optimization was employed to identify combinations of rotor and wing design variables for whirl flutter alleviation, but this study focused on a stiff in-plane tiltrotor configuration (based on a semispan model of the XV-15).

The current effort focuses on soft in-plane tiltrotors. First, a passive design parameter variation study is undertaken to understand the influence of individual rotor/wing design parameters on whirl flutter stability. This is followed by a formal design optimization to identify combinations of design parameters that provide the greatest improvement in aeroelastic stability characteristics in the airplane mode. The Boeing model 222 soft in-plane tiltrotor is used as a baseline for the parametric and optimization studies. Constraints on design parameters during optimization are introduced to prevent unrealistically large changes. However, the effect of relaxing the constraints and opening up the design space to potentially new designs is also examined.

II. Analytical Model

The analytical model used in the present investigation was developed in [31] and is fully documented in [32]. The model represents a proprotor with three or more blades, mounted on a semispan cantilevered wing structure. The wing model is based upon the model developed by Johnson [19]. The wing is represented using only the first three structural modes: vertical bending or beam b, chordwise bending c, and torsion t. Offsets of the wing, pylon, and rotor centers of gravity relative to the wing elastic axis are considered that may couple wing bending and torsion motion.

The point of attachment between the rotor hub and the wing/pylon system can undergo three displacements (x, y, z) and three rotations $(\alpha_x, \alpha_y, \alpha_z)$. The mass, damping, and stiffness properties associated with these degrees of freedom derive from the wing/pylon structure.

The blade is attached to the hub with some precone angle, β_P. Perturbation of rotor azimuthal position in the rotating frame ψ_s is included, allowing a windmilling rotor condition to be modeled. Blade flapping motion β and in-plane lead-lag motion ζ are also included. The rotor aerodynamic model is based on quasi-steady blade element theory and the rotor is assumed to operate in purely axial flow.

Perturbations in blade pitch are related to blade flap, and blade lag motion through aeroelastic coupling parameters:

$$\delta\theta = -K_{P\beta}\beta - K_{P\zeta}\zeta \tag{1}$$

The pitch-flap coupling parameter $K_{P\beta}$ (positive for flap-up, pitch-down) and pitch-lag coupling parameter $K_{P\zeta}$ (positive for lagback, pitch-down) relate changes in blade pitch to blade flap and lag deflections relative to the hub. Potential sources of pitch-flap and pitch-lag coupling in the present analysis will be discussed later.

A. Blade Structural Flap-Lag Coupling Due to Flexibility Distribution

The present analysis models the distribution of blade flexibility inboard and outboard of the pitch bearing, which results in a structural flap-lag coupling (SFLC) of the rotor blades. This formulation has been used previously in helicopter rigid-blade stability analyses [33,34]. Blade flap and lag stiffness is modeled using a set of orthogonal hub springs ($K_{\beta H}$ and $K_{\zeta H}$) inboard of the pitch bearing, and orthogonal blade springs ($K_{\beta B}$ and $K_{\zeta B}$) outboard of the pitch bearing (see Fig. 1a). The relative angle between the hub and blade springs ($\bar{\theta}$) varies as the outboard part of the blade rotates with changes in collective pitch. This series of hub and blade springs may be equivalently described in terms of effective flap and lag flexural stiffnesses K_β and K_ζ and structural flap-lag coupling parameters R_β and R_ζ, which define the distribution of flap and lag flexibility inboard and outboard of the pitch bearing:

$$K_\beta = \frac{K_{\beta H}K_{\beta B}}{K_{\beta H}+K_{\beta B}} \qquad K_\zeta = \frac{K_{\zeta H}K_{\zeta B}}{K_{\zeta H}+K_{\zeta B}} \qquad R_\beta = \frac{K_\beta}{K_{\beta B}} \qquad R_\zeta = \frac{K_\zeta}{K_{\zeta B}} \tag{2}$$

In Eq. (2), a value of $R_\beta = 0$ describes a blade where all the flap flexibility is located inboard of the pitch bearing, and $R_\beta = 1$ represents a blade where all the flap flexibility is outboard of the pitch bearing. The distribution of lag flexibility varies similarly, but with parameter R_ζ. See [34] for a detailed description of this formulation. Tiltrotor aircraft typically experience large changes in blade flap and lag mode frequencies, due to the large changes in collective pitch required to trim the rotor over the entire flight-speed range. By modeling blade stiffness as a series of springs inboard and outboard

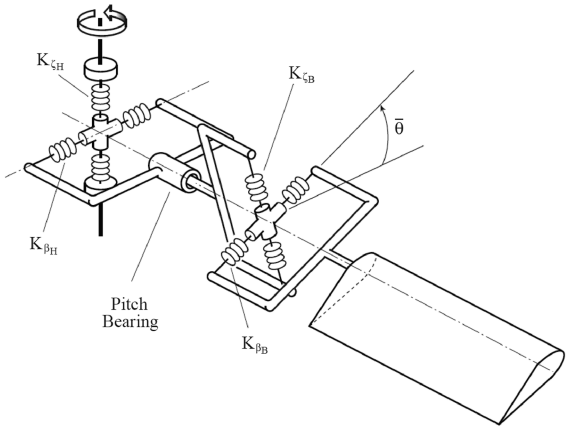

a) Modeling of blade flap/lag flexibility distribution

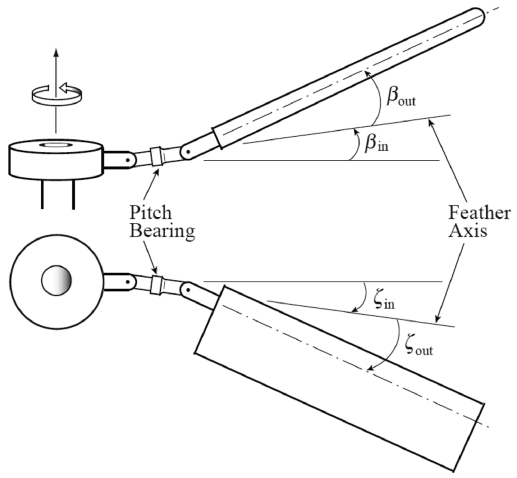

b) Blade flap/lag displacement due to flexibility distribution

Fig. 1 Influence of flap/lag flexibility distribution inboard or outboard of pitch bearing.

of the pitch bearing, the effective blade flap and lag stiffness in the present model becomes a function of collective pitch. Reference [31] showed that by selecting proper values of the effective flatwise and chordwise stiffnesses K_β and K_ζ and coupling parameters R_β and R_ζ, the correct variation of blade flap and lag frequency with collective pitch may be modeled directly. This is unlike many rigid-blade tiltrotor stability analyses, which require blade flap and lag frequency variations be provided explicitly as inputs to the analysis.

B. Pitch-Flap and Pitch-Lag Couplings Due to Blade Flexibility Distribution

The present analysis also includes expressions for pitch-flap and pitch-lag coupling parameters that capture the influence of blade flexibility distribution (inboard /outboard of the pitch bearing) on aeroelastic stability. As described in [20], these couplings act to reduce the whirl flutter stability boundary. References [31,32] contain a detailed derivation of the expressions describing the pitch-flap and pitch-lag couplings due to the distribution of blade flexibility.

Considering the distribution of flap and lag flexibility inboard and outboard of the pitch bearing described in the SFLC formulation above, the total flap and lag displacement of the blade may be defined (assuming small rotations) as the sum of flap and lag displacements inboard and outboard of the pitch bearing. When the blade undergoes flap and lag motions, the feather axis of the blade undergoes a rotation of β_{in} out of plane and ζ_{in} in plane. At the same time, the blade itself undergoes rotations of β_{out} and ζ_{out} relative to the feather axis, as shown in Fig. 1b. The displacement of the blade relative to the feather axis for nonzero β_{out} and ζ_{out} creates a moment arm by which in-plane and out-of-plane forces acting on the blade may create moments about the feather axis, and these moments must be considered when formulating the blade pitch equation of motion.

In [20], the primary consequence of the blade flexibility outboard of the pitch bearing was shown to be the introduction of an effective negative pitch-lag coupling. In [31] expressions for effective pitch-flap and pitch-lag couplings as a result of flexibility outboard of the pitch bearing were developed for the present analysis. The amount of effective coupling is governed by a few key parameters, including the blade pitch control system stiffness, the trim flap and lag deflection of the blades, the fundamental blade flap and lag stiffnesses K_β and K_ζ, blade flexibility distribution R_β and R_ζ, and by the collective pitch setting. See [31,32] for complete details of the derivations of the effective pitch-flap and pitch-lag couplings due to flexibility outboard of the pitch bearing.

In the present analysis, if the effective pitch-flap and pitch-lag couplings due to flexibility outboard of the pitch bearing are denoted as $\tilde{K}_{P\beta}$ and $\tilde{K}_{P\zeta}$, the total pitch-flap and pitch-lag coupling can be represented as

$$K_{P\beta}^{\text{total}} = \tilde{K}_{P\beta} + \Delta K_{P\beta} \qquad K_{P\zeta}^{\text{total}} = \tilde{K}_{P\zeta} + \Delta K_{P\zeta} \tag{3}$$

where the terms $\Delta K_{P\beta}$ and $\Delta K_{P\zeta}$ are additional design variables introduced to represent the influence of other potential sources of pitch-flap and pitch-lag coupling in the rotor blades, such as composite tailoring [21,25], blade c.g. and aerodynamic center offsets [26–29], or advanced blade tip geometries [23]. The influence of these design parameters on whirl flutter stability stems largely from the coupling between blade pitch and flap/lag motions that these parameters introduce. While the present analysis does not attempt to model these sources of pitch-flap and pitch-lag coupling in detail, the parameters $\Delta K_{P\beta}$ and $\Delta K_{P\zeta}$ may serve as a general representation of the couplings arising from any or all of these sources. These parameters can provide an indication of which sense of coupling (positive or negative) is beneficial and whether or not an optimal value of a particular coupling exists or if the coupling's stabilizing influence continually increases as the coupling increases. To provide detailed design guidance for advanced rotor designs, a more sophisticated analysis would be required.

III. Baseline Configuration

The baseline tiltrotor configuration used for simulations in this study is the full-scale, soft in-plane Boeing model 222 rotor on a semispan wing. This soft in-plane hingeless design was tested at NASA Ames Research Center in the early 1970s. Table 1 lists some of the model's important parameters used in the analysis (see [19] for a more complete listing of model properties). Figure 2 shows wing vertical bending mode damping versus airspeed. The present analysis agrees closely with the results from Johnson's elastic blade formulation from [20], and both analyses correlate well with the available experimental data [1]. Figure 3 shows the predicted damping variation of all the modes, as a function of airspeed. The wing vertical bending mode exhibits very low subcritical damping, and whirl flutter instability is encountered at a speed of 390 kt, with the wing chordwise bending mode being the critical mode.

IV. Parametric Variations

Before conducting formal optimization studies, parametric variations in individual design variables are first examined. This provides a good understanding of the influence of individual design variables on whirl flutter stability.

A. Effect of Rotor Design Parameters on Critical Flutter Speed

The following rotor design variables are considered: 1) flatwise bending stiffness, in terms of the nonrotating natural frequency $\omega_{\beta 0}$; 2) chordwise bending stiffness, in terms of the nonrotating natural frequency $\omega_{\zeta 0}$; 3) distribution of blade flatwise bending flexibility R_β; 4) chordwise bending flexibility R_ζ, inboard/outboard of the pitch bearing; 5) blade pitch-flap coupling $\Delta K_{P\beta}$ (in addition to

Table 1 Boeing 222 full-scale model properties and nominal values

Properties	Values
Number of blades N	3
Rotor radius R	13 ft
Lock number γ	4.06
Solidity σ	0.115
Lift-curve slope $C_{l\alpha}$	5.7
Rotor RPM Ω	386 RPM
Rotor	
$\Delta\omega_{\beta 0}$	16.8 rad/s
$\Delta\omega_{\zeta 0}$	32.7 rad/s
R_β	1.0
R_ζ	1.0
$\Delta K_{P\beta}$	0.05
$\Delta K_{P\zeta}$	0.125
$\Delta\omega_\varphi$	210.5 rad/s
Wing	
$\Delta\omega_{q1}$	19.9 rad/s
$\Delta\omega_{q2}$	32.2 rad/s
$\Delta\omega_p$	67.4 rad/s
ΔK_{Pq1}	0
ΔK_{Pq2}	0

pitch-flap coupling $\tilde{K}_{P\beta}$, due to flexibility outboard of the pitch bearing); 6) blade pitch-lag coupling $\Delta K_{P\zeta}$ (in addition to pitch-lag coupling $\tilde{K}_{P\zeta}$, due to flexibility outboard of the pitch bearing); and 7) control system stiffness, expressed in terms of the torsion frequency ω_φ. The nominal values for each of these design variables for the baseline configuration are given in Table 1.

A change in many of the design variables ($\omega_{\beta 0}, \omega_{\zeta 0}, R_\beta, R_\zeta$, and ω_φ) also results in change in pitch-flap and pitch-lag coupling, $\tilde{K}_{P\beta}$ and $\tilde{K}_{P\zeta}$. It is useful, in these cases, to identify whether the change in whirl flutter characteristics from a change in the design parameter is due to a direct influence (such as through a change in modal frequencies and interaction between the rotor and wing modes) or due to the change in pitch-flap and pitch-lag coupling it introduces. Figures 4–12 show the influence of the individual rotor design variables on the whirl flutter speed of the wing vertical bending (beam), chordwise bending and torsion modes. The influence of each design variable is discussed below.

1) The influence of change in flatwise and chordwise bending stiffness is shown in Fig. 4. Change in flatwise bending stiffness has a very small influence on change in critical whirl flutter speed. Reduced chordwise bending stiffness is stabilizing. The increased stability comes almost entirely through a decrease in the magnitude of $\tilde{K}_{P\beta}$ and $\tilde{K}_{P\zeta}$. If $\tilde{K}_{P\beta}$ and $\tilde{K}_{P\zeta}$ are held to their baseline values, changes in chordwise bending stiffness has almost no influence on flutter speed, except for the wing beam mode (which is not the critical mode).

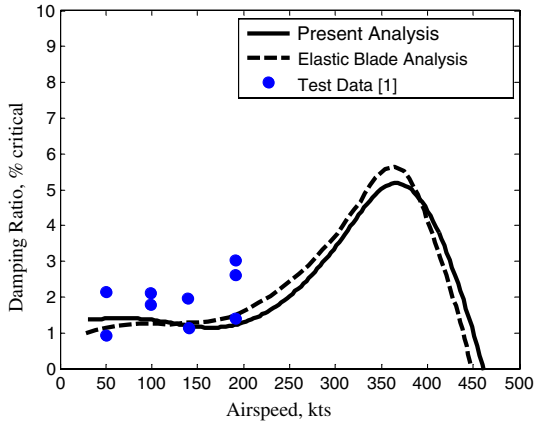

Fig. 2 Boeing model 222: wing vertical bending mode damping vs airspeed.

2) The influence of blade flexibility distribution inboard /outboard of the pitch bearing is examined in Figs. 5–9. Figure 5 shows that as the flatwise flexibility moves inboard of the pitch bearing (R_β decreases from the baseline value of 1), substantial increase in flutter speed is observed. This increase in flutter speed is largely due to the sharp reduction in pitch-flap and pitch-lag coupling. If $\tilde{K}_{P\beta}$ and $\tilde{K}_{P\zeta}$ are artificially held to their baseline values while reducing R_β, there is almost no influence on flutter speed (except in the region where R_β is less than 0.35; flutter speed starts to increase even if $\tilde{K}_{P\beta}$ and $\tilde{K}_{P\zeta}$ are held to their baseline values). Figure 6 shows the modal damping versus airspeed for $R_\beta = 0.6$. Subcritical damping of the wing

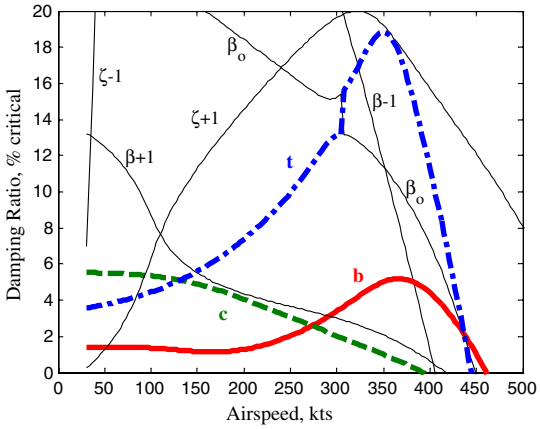

Fig. 3 Baseline modal damping as a function of airspeed.

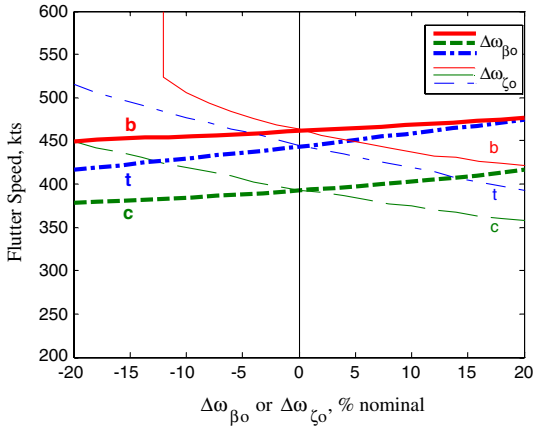

Fig. 4 Influence of blade flatwise and chordwise bending stiffness on flutter speed.

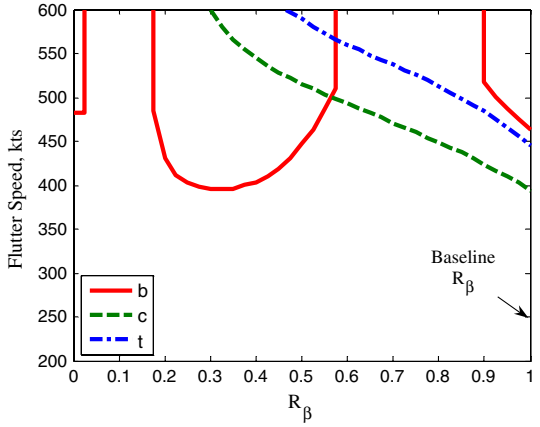

Fig. 5 Influence of distribution of flatwise bending flexibility on flutter speed.

vertical bending (beam) mode remains very low although flutter speed increases by more than 100 kt relative to the baseline.

Moving chordwise flexibility inboard of the pitch bearing (R_ζ reduces from baseline value of 1) has a destabilizing influence on whirl flutter (see Fig. 7). Reduction of R_ζ alone not only introduces destabilizing changes in pitch-flap and pitch-lag coupling but also results in large changes in rotor flap frequencies. The change in pitch-flap coupling is much larger than the change in pitch-lag coupling. However, even when $\tilde{K}_{P\beta}$ and $\tilde{K}_{P\zeta}$ are held to their baseline values, flutter speed still decreases substantially as R_ζ reduces. Thus, frequency change due to reduction in R_ζ also has an influence on flutter speed.

Allowing R_β and R_ζ to vary independently gives you greater design flexibility. However in the extreme cases, such as $R_\beta = 1$, $R_\zeta = 0$ or $R_\beta = 0$, $R_\zeta = 1$, leads to very high blade frequencies. This is shown in Fig. 8. When keeping R_β at 1 and decreasing R_ζ all the way to 0, which means that chordwise flexibility has moved inboard of pitch bearing and the blade chordwise stiffness has reached infinity, this large blade chordwise stiffness results in substantial increase of the blade flatwise stiffness due to large collective pitch angle setting. This is shown in Fig. 8a. Similarly, if R_β is decreased to 0 and while R_ζ remaining at 1 (moving flatwise flexibility inboard of pitch bearing and making the blade flatwise stiffness almost rigid), this large blade flatwise stiffness is transferred into the blade chordwise stiffness because of large collective pitch angle (see Fig. 8b).

Figure 9 shows flutter-speed variations when flatwise and chordwise flexibilities are moving simultaneously. Moving both flatwise and chordwise bending flexibility inboard of pitch bearing ($R_\beta = R_\zeta$, reducing from baseline value of 1) has a stabilizing influence on whirl flutter speed, except in the region where R is less

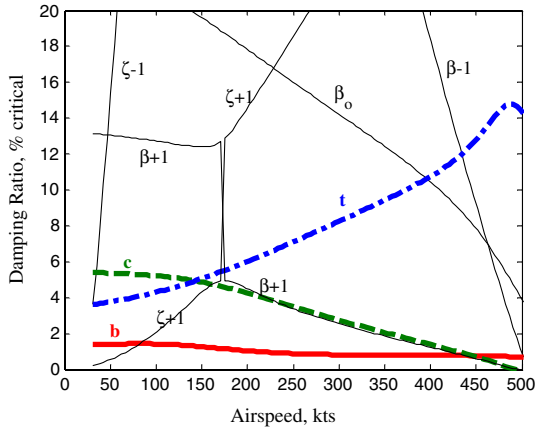

Fig. 6 Damping distribution at $R_\beta = 0.6$ and $R_\zeta = 1.0$.

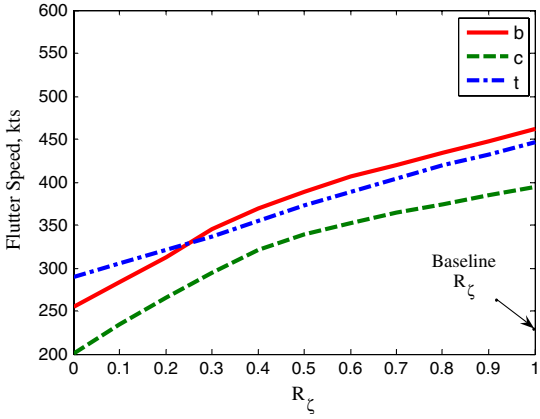

Fig. 7 Influence of distribution of chordwise bending flexibility on flutter speed.

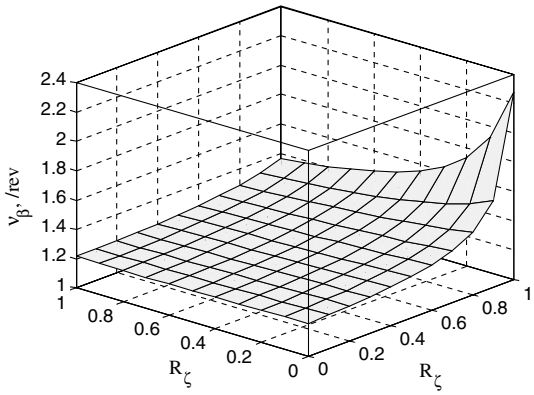

a) ν_β vs. R_β and R_ζ

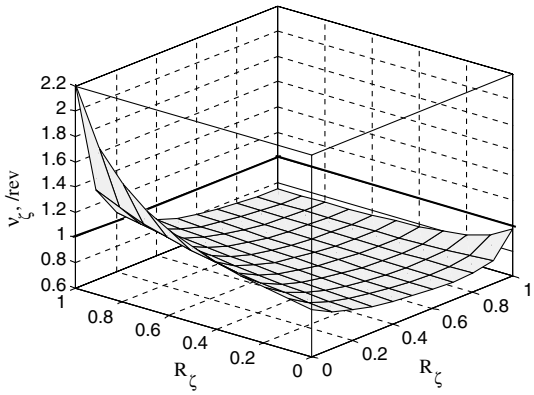

b) ν_ζ vs. R_β and R_ζ

Fig. 8 Rotating flap and lag frequency as a function of R_β and R_ζ.

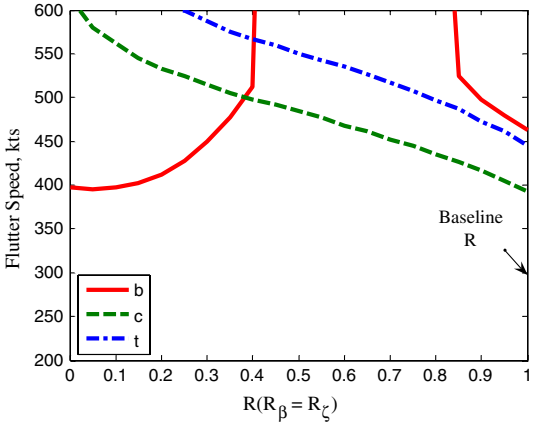

Fig. 9 Influence of flatwise and chordwise bending flexibility ($R_\beta = R_\zeta$) on flutter speed.

than 0.4. The general trend of flutter-speed distributions is similar to that of flatwise bending flexibility change alone (Fig. 5). It is also observed that when R is reduced to 0.4, flutter speed increases by more than 100 kt relative to the baseline. However, subcritical damping of the wing vertical bending (beam) mode remains very low. Modal damping distribution versus airspeed for $R = 0.4$ is almost the same as Fig. 6.

3) The individual influence of pitch-flap coupling, $\Delta K_{P\beta}$, and pitch-lag coupling, $\Delta K_{P\zeta}$, is shown in Figs. 10 and 11, respectively. It should be noted that changes in $\omega_{\beta 0}$, $\omega_{\zeta 0}$, R_β, or R_ζ result in changes $\tilde{K}_{P\beta}$ and $\tilde{K}_{P\zeta}$ simultaneously. From Fig. 10 it is observed that a positive $\Delta K_{P\beta}$ is stabilizing. A positive $\Delta K_{P\zeta}$ shows a stabilizing trend for the wing chord mode, but no increase in flutter speed is observed due to the low-frequency rotor flap mode going unstable (Fig. 11).

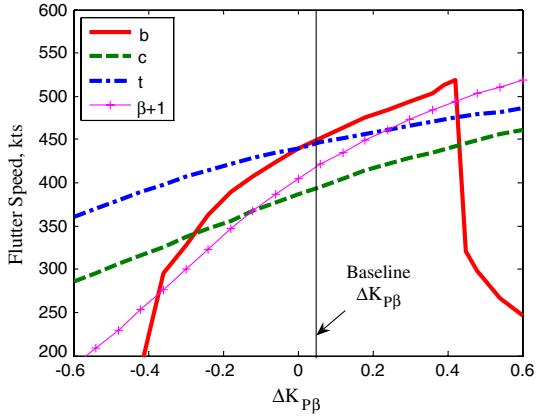

Fig. 10 Influence of additional pitch-flap coupling on flutter speed.

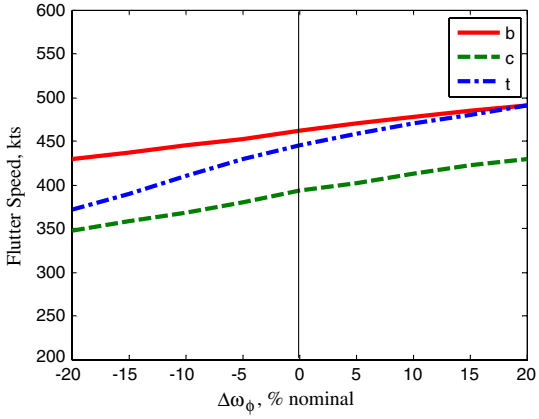

Fig. 12 Influence of control system stiffness on flutter speed.

It should be noted that the stabilizing influence of $\Delta K_{P\beta}$ and $\Delta K_{P\zeta}$ reaches maximum near $+0.4$ and $+0.15$, respectively. At high airspeeds near the flutter boundary, the baseline pitch-flap and pitch-lag coupling, $\tilde{K}_{P\beta}$ and $\tilde{K}_{P\zeta}$, due to flexibility outboard of the pitch bearing is about -0.4 and -0.15. Thus, highest flutter speeds are seen when the positive $\Delta K_{P\beta}$ and $\Delta K_{P\zeta}$ completely offsets the negative contribution from $\tilde{K}_{P\beta}$ and $\tilde{K}_{P\zeta}$.

4) The influence of control system stiffness is presented in Fig. 12. Increase in system stiffness increases the flutter speed, and this is due to the decrease in magnitudes of the pitch-flap and pitch-lag coupling $\tilde{K}_{P\beta}$ and $\tilde{K}_{P\zeta}$. If $\tilde{K}_{P\beta}$ and $\tilde{K}_{P\zeta}$ are held at their baseline values, change in control system stiffness has no influence on the flutter stability boundary.

B. Effect of Wing Design Parameters on Critical Flutter Speed

The wing parameters considered included vertical ω_{q1} and chordwise bending frequency ω_{q2}, torsion frequency ω_p, as well as wing bending-torsion coupling parameters K_{pq1} and K_{pq2}. It should be noted that these elastic coupling parameters may represent wing bending-torsion couplings due to composite tailoring of the wing structure. The vertical bending-torsion coupling parameter K_{pq1} and chordwise bending-torsion coupling parameter K_{pq2} are included in the wing structural stiffness matrix as offdiagonal coupling terms. The wing structural stiffness matrix can then be written as

$$\begin{bmatrix} K_{q1} & 0 & K_{pq1} \\ 0 & K_{q2} & K_{pq2} \\ K_{pq1} & K_{pq2} & K_p \end{bmatrix} \tag{4}$$

where K_{q1}, K_{q2}, and K_p are the fundamental stiffnesses associated with the wing modes.

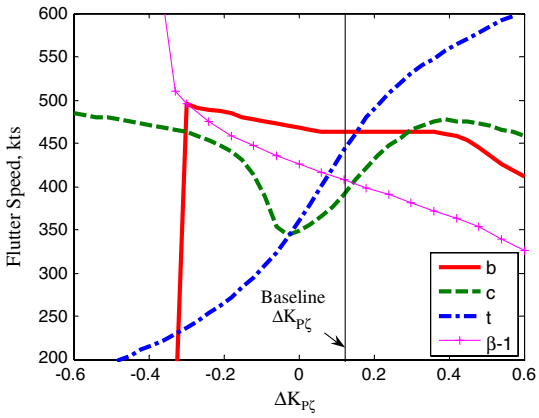

Fig. 11 Influence of additional pitch-lag coupling on flutter speed.

As in the case of the stiff in-plane configuration parametric studies [30], the influence of wing design variables considered in this study on flutter speed is small relative to rotor design parameters.

C. Effect on Subcritical Damping

The effect of various design parameters on change in flutter speed was examined. But one of the key issues that remain is the low subcritical wing beam mode damping, which can be seen in the baseline (Fig. 3). This low subcritical damping in wing beam mode is a phenomenon common to other soft in-plane tiltrotor designs [2]. In Fig. 6 it was observed that variations in rotor parameter R_β that increase critical flutter speed do not improve subcritical damping. In fact, the subcritical damping of wing beam mode deteriorated (compared to the baseline; see Fig. 3). Given that the critical flutter speed of this configuration is already quite high (about 390 kt), and that the subcritical wing beam mode damping is so low, it is certainly interesting to consider what the effect of these various design parameters might be in potentially improving wing beam mode subcritical damping.

Each rotor and wing design parameter was individually varied within the same upper and lower limits as in flutter-speed study, and the effect on wing beam mode damping was examined at airspeeds before the onset of flutter. Most of the design parameters had only a marginal influence on improving wing beam mode damping. Perhaps the only parameter that showed some positive effect on wing beam mode subcritical damping is wing vertical bending frequency ω_{q1}. As seen in Fig. 13, a 20% reduction in wing vertical bending frequency ω_{q1} increases the damping of wing beam mode from 2 to 3.7% at 250 kt airspeed, and from 5 to 10.5% at 350 kt airspeeds. Even though flutter-speed increase is not achievable with wing design variables, the improvement in subcritical damping in poorly

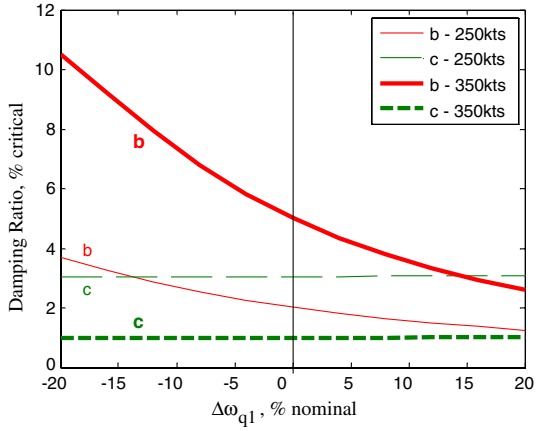

Fig. 13 Influence of wing vertical bending stiffness on subcritical modal damping.

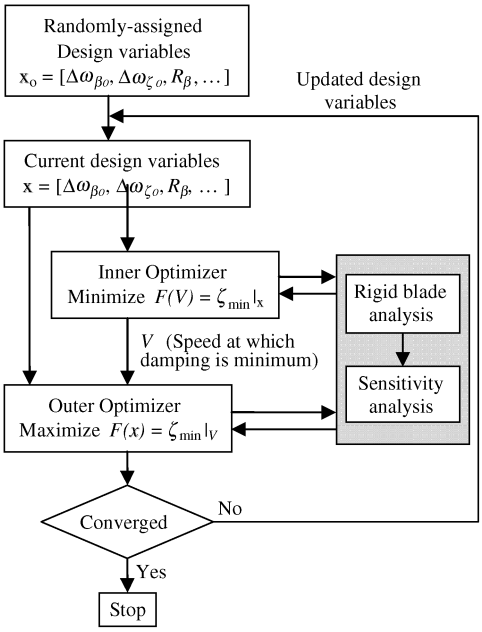

Fig. 14 Moving-point optimization algorithm.

damped wing beam mode positively influences overall stability characteristics.

V. Design Optimization

After performing parametric studies to understand the influence of the individual rotor and wing design parameters on whirl flutter stability (critical flutter speed and subcritical damping of poorly damped wing mode), formal design optimization is conducted to identify optimal combinations of design variables that provide the greatest improvement in aeroelastic stability characteristics: high whirl flutter speeds and reasonable subcritical damping levels in the airplane mode. A gradient-based MATLAB® optimization routine (`FMINCON`) is used to perform the parametric optimization. The algorithm attempts to maximize a user-defined objective function $F(x)$, where x is the vector of design parameters considered in the optimization. For this study, an objective function was formulated to maximize the modal damping of the least damped mode ζ_{min} over preselected airspeed range (nominally between 200 and 500 kt):

$$\text{Maximize } F(x) = \zeta_{min}|_{V=200\rightarrow 500 \text{ kt}} \tag{5}$$

For each iteration of the optimization, using the current set of design variables, the inner optimization loop searches for the airspeed at which the damping is lowest; then the outer optimization iteration is performed at that speed. This two-stage moving-point optimization process continues until the optimal solution (vector of design variables) is determined. Figure 14 shows a flowchart of the two-stage moving-point optimization process.

For the purposes of this optimization study, two sets of constraints on the allowable range of values for the design parameters are considered: relaxed and tight constraints. In an actual tiltrotor design, constraints based on considerations such as weight, allowable loads, handling qualities, and transient rotor flapping would likely prevent the designer from making arbitrarily large changes to the design parameters in order to improve aeroelastic stability.

A small change in any one design parameter may not provide sufficient stability gains. The tight set of constraints is formulated to examine what increases in stability may be obtained through relatively modest changes to many design variables simultaneously. This might be a reasonable approach to improve the aeroelastic stability characteristics of existing configurations. The relaxed constraints further show what additional gains in stability are possible if larger changes to the baseline design are permitted, and they thus open a window to new potential configurations. The two sets of constraints on the design parameters are given in Table 2. Nominal values for each design parameters (corresponding to the Boeing 222 full-scale semispan model) are provided in Table 1.

Table 2 Constraints on design parameters

	Tight constraints	Relaxed constraints
$\Delta\omega_{\beta 0}$	$-5/+5\%$	$-20/+20\%$
$\Delta\omega_{\zeta 0}$	$-5/+5\%$	$-20/+20\%$
R_β	0.8/1.0	0/1.0
R_ζ	0.8/1.0	0/1.0
$\Delta K_{P\beta}$	$-0.1/0.1$	$-0.6/0.6$
$\Delta K_{P\zeta}$	$-0.1/0.1$	$-0.6/0.6$
$\Delta\omega_\varphi$	$-5/+5\%$	$-20/+20\%$
$\Delta\omega_{q1}$	$-5/+5\%$	$-20/+20\%$
$\Delta\omega_{q2}$	$-5/+5\%$	$-20/+20\%$
$\Delta\omega_p$	$-5/+5\%$	$-20/+20\%$
ΔK_{Pq1}	$-0.1/0.1$	$-0.6/0.6$
ΔK_{Pq2}	$-0.1/0.1$	$-0.6/0.6$

A. Rotor Design Optimization

The moving-point optimization process described above was performed, using each of the two previously defined sets of constraints on rotor design parameters. Table 3 provides the resulting values of the optimized rotor design parameters.

The resulting damping characteristics of the optimized configuration with tight constraints are shown in Fig. 15. In this optimized configuration (Table 3), most design parameters have reached their upper or lower limits. Comparing the optimized design to the parametric study results shows that each parameter generally follows the stabilizing trend identified in the parametric studies. Even though the changes allowed to the baseline configuration are small due to the tight bounds on the design parameters, the flutter speed of the optimized configuration is increased by 40 kt over the baseline (Fig. 3), from 390 to 430 kt. The majority of the increase in flutter speed over the baseline is produced by the change in the parameter R_β. If R_β is held at its optimal value and the other variables are returned to their baseline values, the flutter boundary as well as the damping levels in the wing modes are very close to the results in Fig. 15. Although the flutter speed is increased, the very low subcritical damping of the wing beam mode is not improved.

Figure 16 shows the modal damping versus airspeed for the optimized configuration obtained using the relaxed constraints over 200 to 500 kt. When the constraints on the design variables are relaxed, the optimal design is free of whirl flutter over the airspeed range considered (up to 500 kt). In addition, large overall increases in modal damping levels are observed over the range considered

Table 3 Rotor design optimization results

	$\Delta\omega_{\beta 0}$	$\Delta\omega_{\zeta 0}$	R_β	R_ζ	$\Delta K_{P\beta}$	$\Delta K_{P\zeta}$	$\Delta\omega_\varphi$
Tight (200–500 kt)	+5.0%	−5.0%	0.8	1.0	0.1	0.055	+5.0%
Relaxed (200–500 kt)	+20%	+5.4%	0.01	0.88	−0.08	−0.48	+20%
Relaxed (200–500 kt) with ν_ζ constraint	−11%	−20%	0.87	0.64	0.26	0.23	+20%
Relaxed (150–400 kt) with ν_ζ constrain	+20%	+20%	0.73	0.41	0.22	0.29	+13%
Relaxed (150–400 kt) with $R_\beta = R_\zeta$	+20%	+20%	0.86	0.86	0.21	0.30	+20%

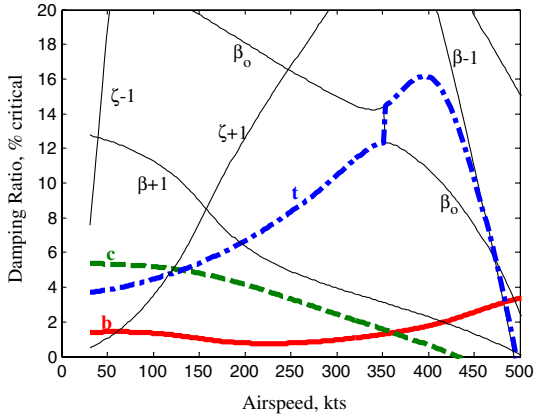

Fig. 15 Rotor design optimization; Maximize damping over 200–500 kt airspeed range under tight constraints.

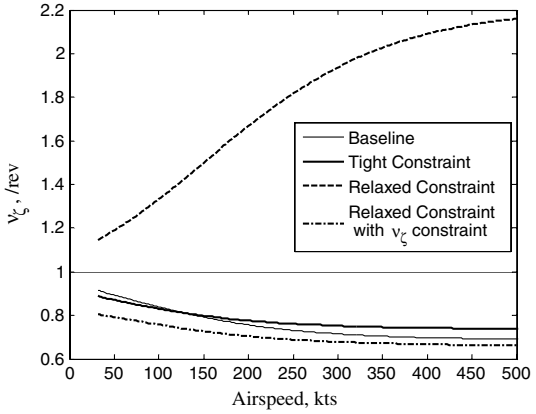

Fig. 17 Rotating lag frequency variations with respect to optimization constraints (tight, relaxed, and relaxed with rotating lag frequency constraint).

(greater than 5% critical damping over the 200–500 kt range considered in the optimization). While some of the design parameters in the optimized configuration have continued following the parametric study trends to their allowable limits, others have not (see Table 3). To examine the importance of each design variable in stability improvement, each parameter is varied individually (from its optimum value), with all the others held at the optimum values. Flatwise and chordwise bending flexibility distributions turn out to be most influential parameters. The optimal design (Table 3) moves the flap flexibility almost entirely inboard relative to the pitch bearing while leaving the lag flexibility mostly outboard of pitch bearing. This change in flexibility distribution is the dominant factor behind the large increase in damping seen in Fig. 16. In fact, by changing R_β to 0 (flap flexibility entirely in the hub), leaving R_ζ at 1 (lag flexibility entirely outboard, in the blade) and all the other design parameters at their baseline values, the resulting modal damping distribution is very similar to that seen in Fig. 16.

When the frequencies for the optimized configuration with relaxed constraints are examined, rotating lag frequency (ν_ζ) of optimum solution is found to be over 1/rev (Fig. 17). This implies that the optimized configuration is not a soft in-plane configuration any more. The optimization problem placed constraints on the design variables and this was expected to be sufficient to bound the rotating lag frequency less than 1/rev. However, for this specific case, when all the flap flexibility moves inboard of the pitch bearing (which implies that the blade has a very high flatwise bending stiffness), high collective pitch setting transfers the high blade flatwise stiffness to the blade lag mode. To avoid the resulting stiff in-plane design that emerges from the optimization process, additional constraints are imposed directly on the rotating lag mode frequency:

$$0.5/\text{rev} < \nu_\zeta < 0.9/\text{rev} \tag{6}$$

Figure 18 shows modal damping characteristics corresponding to the new optimal solution, with ν_ζ constraints (6) active. It is observed that the wing beam mode subcritical damping levels remain very low, even though high flutter speed is achieved. The optimal rotor design with the lag frequency constraint is given in Table 3 and it is observed that R_β is no longer able to move to near-zero values, even though the range for this design parameter goes from 0 to 1. In other words, the lag frequency constraint does not allow all of the flap flexibility to move inboard of pitch bearing.

To overcome the very low subcritical damping of wing vertical bending mode, the optimization process is carried out over a different airspeed range (150–400 kt). The rationale for maximizing the damping over this range has to do with the fact that the baseline Boeing model 222 already has a high critical flutter speed (over 390 kt), while having unacceptably low subcritical wing vertical beam mode damping. Therefore, it would be sufficient to increase the subcritical wing beam mode damping without necessarily increasing critical flutter speed. By considering a large 200–500 kt airspeed range, it may be a challenge for the optimizer to find a design that is stable at the high speed (excess of 400 kt) and simultaneously has good subcritical damping characteristics. So the optimization problem can be restated as the following:

$$\text{Maximize } F(x) = \zeta_{\min}|_{V=150\to400\text{ kt}} \tag{7}$$

with ν_ζ constraints (6) active and with relaxed constraints on design variables shown in Table 2.

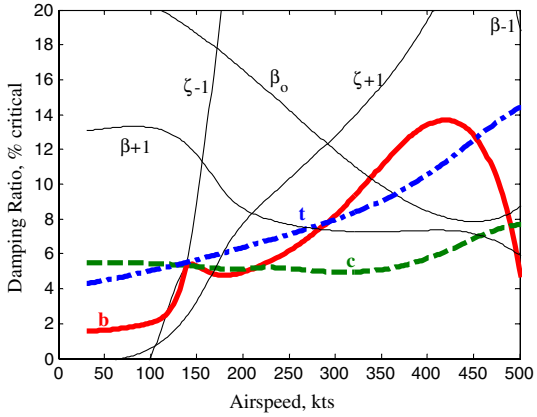

Fig. 16 Rotor design optimization; Maximize damping over 200–500 kt airspeed range under relaxed constraints without rotating lag frequency constraint.

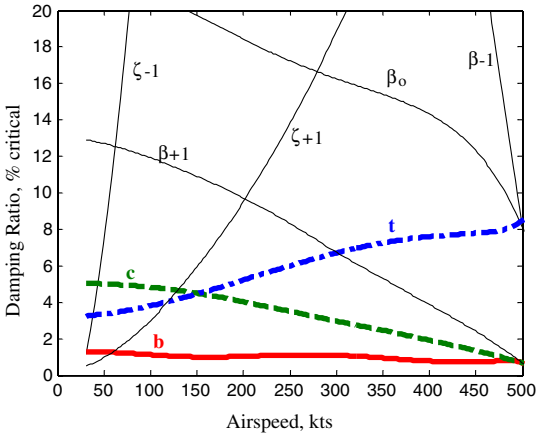

Fig. 18 Rotor design optimization; Maximize damping over 200–500 kt airspeed range under relaxed constraints with rotating lag frequency constraint.

The resulting design is also presented in Table 3 and modal damping behavior versus airspeed is in Fig. 19. A 2% critical minimum damping is maintained over 150 to 400 kt speed range and a 35 kt flutter-speed increase over baseline is still achieved.

Although optimization over the modified airspeed range (150–400 kt), with constraints on the lag frequency, improved stability while ensuring the design was soft in-plane, the optimal flatwise and chordwise flexibilities distributions were found to be $R_\beta = 0.73$ and $R_\zeta = 0.41$. This implies a larger flatwise flexibility outboard of the pitch bearing and a larger chordwise flexibility inboard of the pitch bearing. Although this flexibility distribution is viable, it is worthwhile to examine if comparable stability improvement could be achieved, while flatwise and chordwise flexibility were constrained to move simultaneously relative to the pitch bearing. A modal damping variation of such a design is almost identical to that shown in Fig. 19. Resulting optimal design is found in Table 3. While constraining R_β to be equal to R_ζ, 2% critical damping over considered airspeed range and 32 kt flutter-speed increase are still obtained in addition to satisfying lag frequency requirement.

B. Wing Design Optimization

Optimization of the wing design parameters is conducted next. The optimization was attempted both over 150–400 and 200–500 kt ranges. For both speed ranges, optimization was conducted using both tight and relaxed constraints (Table 4), yet no increase in flutter speed is observed. However, the designs from optimization over 200–500 kt improves subcritical wing beam mode damping (Fig. 20). With both tight as well as relaxed constraints, the wing beam mode frequency hits its lower bound, whereas the wing torsion frequency hits its upper bound, thereby maximizing the separation between these two modes. In addition to reduced wing beam stiffness and increased torsion stiffness, the optimized design also has negative bending-torsion couplings in the wing. However, further analysis indicated that wing beam and torsion stiffness change were the dominant reasons for subcritical wing beam mode damping increase. Even if the other design variables are held at their baseline values, the modal damping results versus airspeed appear very close to those seen in Fig. 20. Since wing chord mode damping shows no sensitivity to wing design variables, a moving-point optimization over 150–400 kt speed range is not successful. Over this range, the wing chord mode is the critical mode, and the optimizer, in a fruitless effort to improve it, actually degrades the wing beam mode damping.

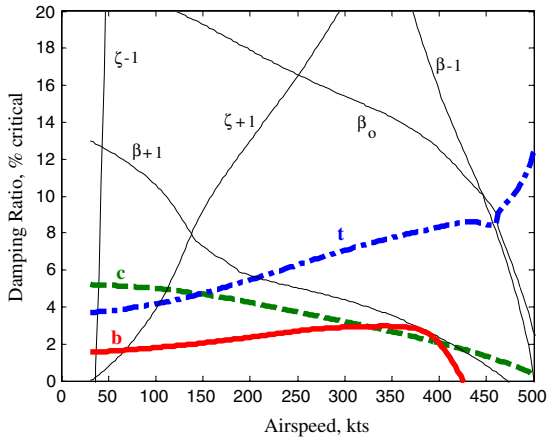

Fig. 19 Rotor design optimization; Maximize damping over 150–400 kt airspeed range under relaxed constraints with rotating lag frequency constraint.

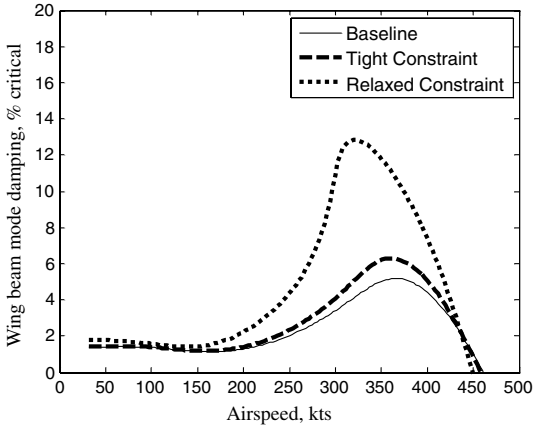

Fig. 20 Wing design optimization; Maximize damping over 200–500 kt airspeed under tight and relaxed constraints.

Table 4 Wing design optimization results

	$\Delta\omega_{q1}$	$\Delta\omega_{q2}$	$\Delta\omega_p$	ΔK_{Pq1}	ΔK_{Pq2}
Tight (150–400 kt)	+5.0%	−5.0%	+5.0%	−0.1	−0.1
Tight (200–500 kt)	−5.0%	+5.0%	+5.0%	−0.1	−0.1
Relaxed (150–400 kt)	+20%	−20%	+20%	−0.6	−0.6
Relaxed (200–500 kt)	−20%	+20%	+20%	−0.6	−0.6

C. Rotor/Wing Design Optimization

Since rotor design optimization and wing design optimization each had certain beneficial effects, the question that was posed was, "What is the effect of combining the optimal rotor design solution and the optimal wing design solution?" When the optimal rotor design (determined using relaxed constraints, lag frequency active, and over a 150–400 kt range, modal damping results in Fig. 19) and the optimal wing design (relaxed constraints, over a 200–500 kt range, modal damping results in Fig. 20) are simply combined, the resulting modal damping characteristics versus airspeed is shown in Fig. 21. Although the subcritical damping levels are reasonable, the critical whirl flutter speed using such a sequential optimization procedure actually reduces to 350 kt (down from 390 kt).

Next, concurrent optimization of rotor-wing design parameters is examined, with relaxed constraints on both sets of parameters and with lag frequency constraint active. Again, the objective function is to maximize the damping of the least damped mode over a 150–400 kt airspeed range. The optimal design is presented in Table 5, and the modal damping versus airspeed results are shown in Fig. 21. Compared to optimization of the rotor variables alone (Fig. 19), a further increase in subcritical beam mode damping levels is observed (especially over the 200–400 kt range). The rotor parameters in the optimal design follows the general trends observed in the parametric studies section, but the wing parameters show differences. Specifically, the reduction in wing beam mode frequency and increase in wing torsion frequency previously observed, is reversed.

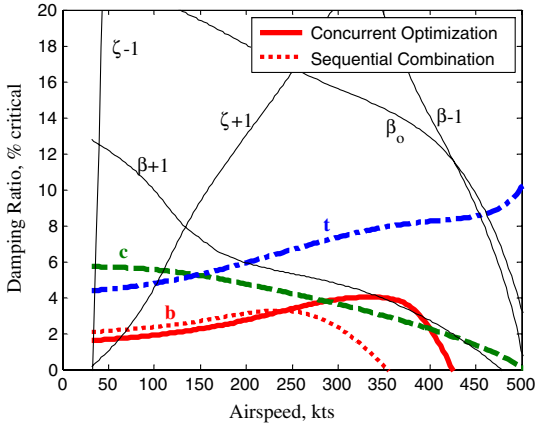

Fig. 21 Sequential combination of rotor and wing optimal designs vs concurrent rotor/wing design optimization (over 200–500 kt airspeed range under relaxed constraints with rotating lag frequency constraint).

Table 5 Rotor/wing design (concurrent) optimization

$\Delta\omega_{\beta 0}$	$\Delta\omega_{\zeta 0}$	R_β	R_ζ	$\Delta K_{P\beta}$	$\Delta K_{P\zeta}$	$\Delta\omega_\varphi$	$\Delta\omega_{q1}$	$\Delta\omega_{q2}$	$\Delta\omega_p$	$\Delta\omega_{Pq1}$	$\Delta\omega_{Pq2}$
Relaxed 150–400 kt *with* v_ζ *constraint*											
+20%	+20%	0.92	0.78	0.28	0.29	+17%	+20%	−20%	−16%	0.54	−0.6
Relaxed (150–400 kt) *with* $R_\beta = R_\zeta$											
+20%	+20%	0.82	0.82	0.21	0.27	+17%	−16%	+20%	−20%	0.6	−0.6

When flatwise and chordwise bending flexibility are moving simultaneously, almost the same stability improvements (over 2% critical damping over considered airspeed range and 40 kt flutter-speed increase) are achievable, compared to the result of Fig. 21. The optimal design for this case is presented in Table 5.

VI. Conclusions

An analytical investigation of the influence of various rotor and wing design parameters on soft in-plane tiltrotor whirl flutter stability was conducted. The baseline tiltrotor configuration used in the study was the full-scale soft in-plane Boeing model 222 rotor on a semispan wing. The influence of parametric changes in individual design variables on flutter speed was considered first. Formal gradient-based optimization was then used in order to identify combinations of design parameters that would increase the critical whirl flutter speed and improve the subcritical modal damping levels, especially in the poorly damped wing vertical bending mode. The process of formulating a properly posed optimization problem in order to achieve the desired stability characteristics is examined, as is the effect of tight versus relaxed constraints on design variables, and additional rotating frequency constraints. Optimization is conducted for rotor parameters only, wing parameters only, and the two sets considered together.

The main conclusions drawn from this study are summarized below.

1) Of the rotor parameters considered, the most influential is the flatwise flexibility distribution relative to the pitch bearing. For the baseline model 222 configuration, the flatwise flexibility was all outboard of the pitch bearing and the hub was rigid. This introduces destabilizing negative pitch-flap and pitch-lag couplings. Moving some of the flexibility inboard of the pitch bearing reduces the destabilizing couplings and increases the flutter speed. However, it should be noted that if a substantial portion of the flatwise flexibility is moved inboard of the pitch bearing, although it can produce large benefits in flutter speed and subcritical wing mode damping increases, the blade is now stiff in flatwise bending, and the high collective angle transfers a large part of that stiffness into the lag mode. The resulting designs tend to be stiff in-plane designs. When frequency constraints are placed on the lag mode during optimization to alleviate this problem, only a small amount of flatwise flexibility can move inboard of the pitch bearing, and the improvements seen are much more modest.

2) Other rotor parameter changes that have benefits in terms of flutter-speed increase are reduction in rotor overall chordwise stiffness, a positive increase in pitch-flap and pitch-lag coupling, and an increase in control system stiffness.

3) With tight constraints on the design variables, an optimized design increases flutter speed but does not increase the subcritical damping. The optimizer produces generally intuitive results in that the optimal combination of design parameters follow trends identified by varying design parameters individually.

4) With relaxed constraints on the design variables, lag frequency constraint, and a proper selection of airspeed range over which optimization is conducted, a modest increase in subcritical wing beam mode damping can be achieved (from a very low level of less than 1% to levels in excess of 2% critical), in addition to an increase in critical flutter speed.

5) Constraining flatwise and chordwise flexibility distributions to move simultaneously relative to the pitch bearing can achieve comparable stability improvement to that from moving flatwise and chordwise flexibility independently with the rotating lag frequency constraint either in rotor design or in rotor/wing design concurrent optimization and also successfully maintain the rotating lag frequency less than 1/rev.

6) In general, wing design parameters are less influential than the rotor design parameters. They are unable to increase the critical flutter speed because damping in the wing chord mode, which is the critical mode, is uninfluenced by the wing design parameters. However, increasing the wing torsion frequency and simultaneously reducing the wing vertical bending mode frequency (thereby increasing the frequency separation) appears to increase the subcritical damping levels in the wing beam mode. Wing bending-torsion couplings also appear to play a role, albeit a smaller one.

7) Concurrent optimization of rotor/wing design variables is able to increase flutter speed up from 390 to 425 kt and provides over 2% critical of subcritical wing beam mode damping (further improvement compared to that observed from the rotor design only optimization) relative to the level of less than 1% critical of baseline configuration.

Acknowledgments

This project was funded by the Center for Rotorcraft Innovation (CRI) and the National Rotorcraft Technology Center (NRTC), U.S. Army Aviation and Missile Research, Development and Engineering Center (AMRDEC) under Technology Investment Agreement W911W6-06-2-0002, entitled National Rotorcraft Technology Center Research Program. The authors would like to acknowledge that this research and development was accomplished with the support and guidance of the NRTC and CRI. The views and conclusions contained in this document are those of the authors and should not be interpreted as representing the official policies, either expressed or implied, of the AMRDEC or the U.S. Government. The U.S. Government is authorized to reproduce and distribute reprints for Government purposes notwithstanding any copyright notation thereon.

References

[1] Magee, J. P., and Alexander, H. R., "Wind Tunnel Tests of a Full Scale Hingeless Prop/Rotor Designed for the Boeing Model 222 Tilt Rotor Aircraft," NASA CR 114664, Oct. 1973.

[2] Nixon, M. W., Langston, C. W., Singleton, J. D., Piatak, D. J., Kvaternik, R. G., Corso, L. M., and Brown, R. K., "Aeroelastic Stability of a Four-Bladed Semi-Articulated Soft-Inplane Tiltrotor Model," *AHS International 59th Annual Forum Proceedings* [CD-ROM], AHS International, Alexandria, VA, May 2003.

[3] Nixon, M. W., Piatak, D. J., Corso, L. M., and Popelka, D. A., "Aeroelastic Tailoring for Stability Augmentation and Performance Enhancement of Tiltrotor Aircraft," *AHS International 55th Annual Forum Proceedings* [CD-ROM], AHS International, Alexandria, VA, May 1999.

[4] Johnson, W., "Optimal Control Alleviation of Tilting Proprotor Gust Response," *Journal of Aircraft*, Vol. 14, No. 3, March 1977, pp. 301–308.
doi:10.2514/3.44594

[5] Nasu, K.-I., "Tilt-Rotor Flutter Control in Cruise Flight," NASA TM 88315, Dec. 1986.

[6] van Aken, J. M., "Alleviation of Whirl Flutter on Tilt-Rotor Aircraft Using Active Controls," *Proceedings of the 47th Annual AHS Forum* [CD-ROM], AHS International, Alexandria, VA, May 1991.

[7] van Aken, J. M., "Alleviation of Whirl Flutter on a Joined-Wing Tilt-Rotor Aircraft Configuration Using Active Controls," *The International Specialists' Meeting on Rotorcraft Basic Research of the American Helicopter Society* [CD-ROM], AHS International, Alexandria, VA, March 1991.

[8] Kvaternik, R. G., Piatak, D. J., Nixon, M. W., Langston, C. W., Singleton, J. D., Bennett, R. L., and Brown, R. K., "An Experimental Evaluation of Generalized Predictive Control for Tiltrotor Aeroelastic Stability Augmentation in Airplane Mode of Flight," *Proceedings of the 57th Annual AHS Forum* [CD-ROM], AHS International, Alexandria, VA, May 2001.

[9] Nixon, M. W., Langston, C. W., Singleton, J. D., Piatak, D. J., Kvaternik, R. G., Corso, L. M., and Brown, R., "Aeroelastic Stability of a Soft-Inplane Gimballed Tiltrotor Model in Hover," *Proceedings of the 42nd AIAA/ASME/ASCE/AHS/ ASC Structures, Structural Dynamics, and Materials Conference*, Seattle, WA, April 2001.

[10] Nixon, M. W., Langston, C. W., Singleton, J. D., Piatak, D. J., Kvaternik, R. G., Corso, L. M., and Brown, R. K., "Hover Test of a Soft-Inplane Gimballed Tiltrotor Model," *Journal of the American Helicopter Society*, Vol. 48, No. 1, Jan. 2003, pp. 63–66. doi:10.4050/JAHS.48.63

[11] Kvaternik, R. G., "Exploratory Studies in Generalized Predictive Control for Active Aeroelastic Control of Tiltrotor Aircraft," NASA TM-2000-210552, 2000.

[12] Hathaway, E., and Gandhi, F., "Tiltrotor Whirl Flutter Alleviation Using Actively Controlled Wing Flaperons," *AIAA Journal*, Vol. 44, No. 11, Nov. 2006, pp. 2524–2534. doi:10.2514/1.18428

[13] Paik, J., Singh, R., Gandhi, F., and Hathaway, E., "Active Tiltrotor Whirl Flutter Stability Augmentation using Wing-Flaperon and Swashplate Actuation," *Journal of Aircraft*, Vol. 44, No. 5, Sept.–Oct. 2007, pp. 1439–1446. doi:10.2514/1.20234

[14] Singh, R., Hathaway, E. L., and Gandhi, F., "Wing-Flaperon and Swashplate Control for Whirl Flutter Stability Augmentation of a Soft-Inplane Tiltrotor," *31st European Rotorcraft Forum (Dynamics Session)*, Florence, Italy, Sept. 2005.

[15] Hall, W. E., Jr., "Prop-Rotor Stability at High Advance Ratios," *Journal of the American Helicopter Society*, Vol. 11, No. 2, April 1966, pp. 11–26.

[16] Young, M. I., and Lytwyn, R. T., "The Influence of Blade Flapping Restraint on the Dynamic Stability of Low Disk Loading Propeller-Rotors," *Journal of the American Helicopter Society*, Vol. 12, No. 4, Oct. 1967, pp. 38–54. doi:10.4050/JAHS.12.38

[17] Wernicke, K. G., and Gaffey, T. M., "Review and Discussion of 'The Influence of Blade Flapping Restraint on the Dynamic Stability of Low Disk Loading Propeller-Rotors'," *Journal of the American Helicopter Society*, Vol. 12, No. 4, Oct. 1967, pp. 55–60. doi:10.4050/JAHS.12.55

[18] Gaffey, T. M., Yen, J. G., and Kvaternik, R. G., "Analysis and Model Tests of the Proprotor Dynamics of a Tilt-Proprotor VTOL Aircraft," *Air Force V/STOL Technology and Planning Conference*, Las Vegas, NV, Sept. 1969.

[19] Johnson, W., "Dynamics of Tilting Proprotor Aircraft in Cruise Flight," NASA TN D-7677, 1974.

[20] Johnson, W., "Analytical Modeling Requirements for Tilting Proprotor Aircraft Dynamics," NASA TN D-8013, 1975.

[21] Nixon, M. W., "Aeroelastic Response and Stability of Tiltrotors with Elastically-Coupled Composite Rotor Blades," Ph.D. Thesis, Univ. of Maryland, College Park, MD, 1993.

[22] Moore, M. J., Yablonski, M. J., Mathew, B., and Liu, J., "High Speed Tiltrotors: Dynamics Methodology," *AHS International 49th Annual Forum Proceedings* [CD-ROM], AHS International, Alexandria, VA, May 1993.

[23] Srinivas, V., Chopra, I., and Nixon, M., "Aeroelastic Analysis of Advanced Geometry Tiltrotor Aircraft," *Journal of the American Helicopter Society*, Vol. 43, No. 3, July 1998, pp. 212–221. doi:10.4050/JAHS.43.212

[24] Popelka, D. A., Lindsay, D., Parham, T., Jr., Berry, V., and Baker, D. J., "Results of an Aeroelastic Tailoring Study for a Composite Tiltrotor Wing," *Journal of the American Helicopter Society*, Vol. 42, No. 2, April 1997, pp. 126–136. doi:10.4050/JAHS.42.126

[25] Barkai, S. M., and Rand, O., "The Influence of Composite Induced Couplings on Tiltrotor Whirl Flutter Stability," *Journal of the American Helicopter Society*, Vol. 43, No. 2, April 1998, pp. 133–145. doi:10.4050/JAHS.43.133

[26] Acree, C. W., Jr., Peyran, R. J., and Johnson, W., "Rotor Design for Whirl Flutter: An Examination of Options for Improving Tiltrotor Aeroelastic Stability Margins," *AHS International 55th Annual Forum Proceedings* [CD-ROM], AHS International, Alexandria, VA, May 1999.

[27] Acree, C. W., Jr., Peyran, R. J., and Johnson, W., "Improving Tiltrotor Whirl Mode Stability with Rotor Design Variables," 26th European Rotorcraft Forum, Paper 14, Hague, The Netherlands, Sept. 2000.

[28] Acree, C. W., Jr., "Effects of Rotor Design Variations on Tiltrotor Whirl Mode Stability," *Tiltrotor/Runway Independent Aircraft Technology & Applications Specialists' Meeting* [CD-ROM], AHS International, Alexandria, VA, March 2001.

[29] Acree, C. W., Jr., "Rotor Design Options for Improving V-22 Whirl Mode Stability," *AHS International 58th Annual Forum Proceedings* [CD-ROM], AHS International, Alexandria, VA, June 2002.

[30] Hathaway, E. L., and Gandhi, F., "Design Optimization for Improved Tiltrotor Whirl Flutter Stability," *Journal of the American Helicopter Society*, Vol. 52, No. 2, April 2007, pp. 79–89. doi:10.4050/JAHS.52.79

[31] Hathaway, E. L., and Gandhi, F., "Modeling Refinements in Simple Tiltrotor Whirl Flutter Analyses," *Journal of the American Helicopter Society*, Vol. 48, No. 3, July 2003, pp. 186–198. doi:10.4050/JAHS.48.186

[32] Hathaway, E. L., "Active and Passive Techniques for Tiltrotor Aeroelastic Stability Augmentation," Ph.D. Thesis, Pennsylvania State Univ., University Park, PA, 2005.

[33] Ormiston, R. A., and Hodges, D. H., "Linear Flap-Lag Dynamics of Hingeless Helicopter Rotor Blades in Hover," *Journal of the American Helicopter Society*, Vol. 17, No. 2, April 1972, pp. 2–14. doi:10.4050/JAHS.17.2

[34] Gandhi, F., and Hathaway, E., "Optimized Aeroelastic Couplings for Alleviation of Helicopter Ground Resonance," *Journal of Aircraft*, Vol. 35, No. 4, 1998, pp. 582–590. doi:10.2514/2.2341